NASA Technical Memorandum 100672

A MAGNETIC BEARING CONTROL APPROACH USING FLUX FEEDBACK

Nelson J. Groom

March 1989

SUMMARY

A magnetic bearing control approach using flux feedback is described and test results for a laboratory model magnetic bearing actuator are presented. Test results were obtained using a magnetic bearing test fixture, which is also described. The magnetic bearing actuator consists of elements similar to those used in a laboratory test model Annular Momentum Control Device (AMCD).

INTRODUCTION

This paper describes a magnetic bearing control approach which uses flux feedback to produce a linear transfer characteristic between force command and force output over a large gap range. An overview of prior related efforts in this area, which led to the present approach, is also presented. The feedback signal is generated by a Hall effect device which is mounted on the pole face of each magnetic bearing actuator element. The approach was initially investigated for application to a laboratory model Annular Momentum Control Device (AMCD). The basic concept of the AMCD is that of a rotating annular rim, suspended by a minimum of three magnetic bearing suspension stations, and driven by a noncontacting electromagnetic spin motor. A detailed discussion of the rationale for the AMCD configuration and some of its potential applications is presented in reference 1. The laboratory model (described in refs. 2 and 3) was built to investigate potential problem areas in implementing the AMCD concept for large radial dimensions.

The magnetic bearing control approach used in the original laboratory model AMCD magnetic suspension was to differentially control sets of magnetic bearing elements about a permanent-magnet bias flux (ref. 2). Early tests indicated that this approach (permanent-magnet flux biasing) imposed constraints on the suspension control system design (ref. 4). As a result, alternate control and linearization approaches have been investigated. These approaches, which will subsequently be discussed in more detail, include an analog solution of the force equation for individual element control (ref. 5) and a microprocessor-based table lookup approach for individual element control (ref. 6).

In a related effort, a variation of the permanent-magnet flux bias approach was developed for the magnetic suspension of the Annular Suspension and Pointing System (ASPS). The ASPS, which is a general-purpose pointing mount designed to provide orientation, mechanical isolation, and fine pointing for space experiments, is a derivative of the AMCD and uses a similar magnetic bearing design and suspension technique (ref. 7). In the ASPS suspension the bias flux is provided by bias currents. The bias currents and control currents are functions of gap displacement in order to provide linear actuator characteristics over a wide gap range. For an overview of magnetic bearing control and linearization approaches for annular magnetically suspended devices, see reference 8.

The flux feedback approach described in this paper allows the use of permanent magnet flux biasing to be used in a magnetic bearing actuator with linear characteristics over a wide gap range without the disadvantages of the original permanent magnet flux bias approach.

1

MAGNETIC BEARING FORCE EQUATIONS

In order to define the basic type of magnetic bearing actuator which will be discussed in this paper, the simplified schematic of figure 1 is introduced. Upper and lower electromagnets with currents I_u and I_L, produce forces F_u and F_L on a suspended element positioned between the electromagnets at a gap distance G_o from the top electromagnet pole face. Since an electromagnet of the type being discussed produces an attractive force only, two are required to produce a bidirectional force capability. A position sensor is shown which measures the displacement G_s of the suspended element with respect to the centered position G_o. Position information is required for active control of the suspended element and is also required for some of the linearization approaches to be discussed.

Single Element

The equations presented in this section are developed in more detail in reference 9. Simplifying assumptions include infinite permeability for the magnetic core material, negligible flux fringing, and negligible flux leakage. If up is taken as the positive direction in figure 1, then the electromagnet gaps become

$$G_u = G_o - G_s \tag{1}$$

and

$$G_L = G_o + G_s \tag{2}$$

From reference 9, the force produced by a single element as a function of current and gap can be written as

$$F = \frac{\mu_o A(NI)^2}{4G^2} \tag{3}$$

where μ_o is the permeability of free space, A is the cross sectional area of the magnetic bearing element core, N is the number of turns in the electromagnet winding, I is current, and G is the magnetic bearing element gap. Since μ_o, A, and N are constants, equation (3) can be written as

$$F = \frac{KI^2}{G^2} \tag{4}$$

where

$$K = \frac{\mu_o AN^2}{4} \tag{5}$$

2

Using the assumption of no leakage flux, the flux in the bearing element gap is equal to the flux in the bearing element core and can be written as

$$\phi = \frac{\mu_o NIA}{2G} \tag{6}$$

Force as a function of flux is obtained by substituting equation (6) into equation (3) which results in

$$F = \left(\frac{1}{\mu_o A}\right)\phi^2 \tag{7}$$

Equation (7) can be written as

$$F = \tilde{K}\,\phi^2 \tag{8}$$

where

$$\tilde{K} = \frac{1}{\mu_o A} \tag{9}$$

Individual Element Control and Linearization Approaches.- As mentioned in the introduction, single element control involves controlling either the upper or lower electromagnet, shown in figure 1, depending on the direction of the force required. Controlling the electromagnets in this way results in a highly nonlinear force current characteristic. This is illustrated by figure 2, which shows the composite force-current characteristic of a magnetic actuator with individual element control and with the suspended mass centered in the actuator gaps. It should be noted that this curve is based on ideal assumptions and, that in practice, the smooth crossover at zero is difficult to achieve because of hardware considerations.

Two linearization approaches have been investigated for individual element control. One approach, which has been implemented for the laboratory model AMCD, utilizes the analog solution of the force equation for a given element. Figure 3 is a simplified block diagram of this implementation which uses analog multipliers and square root modules. The equations for upper and lower elements are included in the figure. A detailed description of this implementation is given in reference 10. This approach proved to be highly sensitive to bearing element calibration and alignment accuracy.

The other linearization approach investigated for individual element control is microprocessor-based and uses a table lookup to generate control signals. This approach was bench tested, but has not been used in the AMCD laboratory model suspension system to date. Figure 4 is a block diagram representation of the laboratory implementation. In this approach, actual calibration data for a given bearing element pair are used to build a lookup table which is stored in the memory of a microprocessor system. Using the force command and gap position as input data, the

correct value of current input to the coil, for the suspended element centered in the actuator gaps, is obtained by using a table lookup routine. This current is compensated for displacement from center by multiplying by the calculated gap. This approach is described in more detail and test results presented in reference 6.

Bias Flux

Permanent Magnet.- As discussed in the introduction, the original control approach used for the laboratory model AMCD magnetic actuators utilized permanent magnet flux biasing. The operation of a permanent magnet flux-biased magnetic actuator can be described by referring to figure 5. This figure is a simplified schematic which shows a single actuator, for control along a single axis, which consists of a pair of magnetic bearing elements with permanent magnets mounted in the cores. The bearing elements are shown connected in a differential configuration. That is, for a given input the amplifier driver shown in the figure produces current in a direction to aid the permanent-magnet-produced flux in one element while at the same time producing equal current in a direction to substract from the permanent-magnet-produced flux in the other element. This results in a net force produced on the suspended mass in a direction dependent on the polarity of the input to the amplifier driver. The force produced by this type actuator as a function of current and gap can be written as (from ref. 9)

$$F = \frac{K_1}{4}\left(\frac{\left[I_o + I\right]^2}{\left[\bar{x}_o - G\right]^2} - \frac{\left[I_o - I\right]^2}{\left[\bar{x}_o + G\right]^2}\right) \tag{10}$$

where K_1, $\bar{x}_o$, and I_o are constants (defined in ref. 9). I_o can be thought of as an equivalent constant bias current provided by the permanent magnets. Figure 6 shows the composite force-current characteristic of this type actuator with the suspended mass centered in the gaps. This figure illustrates a linear actuator gain at a given gap position. By performing a first-order linearization of equation (10) about a fixed operating point, the actuator force as a function of differential coil current and displacement can be written as

$$F = K_B I + K_M G \tag{11}$$

where K_B is an equivalent electromagnet gain and K_M is an equivalent bias flux stiffness (for more detail see ref. 9). These gains would be different for different operating points.

Variable Bias Current.- As mentioned in the introduction, a variation of the permanent magnet flux bias approach was developed for the ASPS in order to provide a linear actuator characteristic over a wide gap range. This approach uses variable bias currents to provide the bias flux. Figure 7 is a simplified block diagram of the variable bias current approach that was implemented for the ASPS. As can be seen by working through the block diagram, the bias current and control currents of the upper and lower electromagnets are adjusted so that the bias force produced by each and the net force produced by a given command force are equal no matter where the suspended

4

mass is in the gap. The unbalanced bias flux stiffness is thus eliminated and the electromagnet gain is constant. A detailed description of this implementation is given in reference 11.

FLUX FEEDBACK APPROACH

When considering simplicity, efficiency, and controllability of force around zero, the permanent magnet flux bias approach trades off better than the other magnetic bearing control and linearization approaches which were discussed in the previous sections. Disadvantages of this approach include a minimum bandwidth requirement for stability (ref. 4) and linear operation over a restricted gap range about a fixed operating point. The variable bias current approach used in the ASPS suspension system was developed to overcome these disadvantages. However, since current is the controlled variable, the implementation of this approach is relatively complicated and requires actuator core material and rotor material with very low hysteresis in order to provide a sufficiently accurate force-output to force-command transfer characteristic (ref. 11). By using flux feedback, the complex current calculation, with the attendant requirement for gap compensation, is no longer required. In addition, the nonlinear transfer characteristic between electromagnet coil current and flux is included in the forward loop of a feedback system with very high open loop gain. This reduces the sensitivity of the force-output to force-input transfer characteristic to a negligible level as long as the actuator is operated below the saturation flux density of the electromagnet core material and rotor material. Bias flux can be supplied by either fixed bias currents or permanent magnets in the flux feedback approach. Test results are presented for a flux feedback implementation which utilizes bias currents. This is due primarily to the fact that there is more flexibility in setting test parameters with bias currents. However, since the data presented are for fixed bias currents, it is directly applicable to an actuator with permanent magnet flux biasing.

Force Equations

The force produced by a given magnetic bearing element as a function of flux in the bearing gap is given by equation (8). Using figure 1 and associated nomenclature again, the force produced by the upper and lower elements becomes

$$F_u = \bar{K}\phi_u^2, \quad F_L = \bar{K}\phi_L^2 \tag{12}$$

For a bearing element pair with differential control of flux, the total force becomes

$$F_T = F_u - F_L \tag{13}$$

which becomes

$$F_T = \bar{K}\left(\phi_u^2 - \phi_L^2\right) \tag{14}$$

5

With differential control about a bias flux, ϕ_o, the flux in the upper and lower gaps become

$$\phi_u = \phi_o + \phi_c \tag{15}$$

$$\phi_L = \phi_o - \phi_c \tag{16}$$

where ϕ_c is flux command. Substituting equations (15) and (16) into equation (14) results in

$$F_T = \bar{K}\left(\left[\phi_o^2 + 2\phi_o\phi_c + \phi_c^2\right] - \left[\phi_o^2 - 2\phi_o\phi_c + \phi_c^2\right]\right) \tag{17}$$

which simplifies to

$$F_T = 4\bar{K}\phi_o\phi_c \tag{18}$$

By making the following definitions

$$\phi_c = F_c \tag{19}$$

$$4\bar{K}\phi_o = K_F \tag{20}$$

the total actuator force output, F_T, as a function of command force input, F_c, becomes

$$F_T = K_F F_c \tag{21}$$

Hardware Configuration

An implementation of the flux feedback approach which uses bias currents is shown in figure 8. The basic approach for the flux feedback loop is to include the bearing element power driver and flux sensor and associated amplifier in the feedback loop of an operational amplifier. A TL3103C linear Hall-effect sensor was used as the flux sensor and was mounted in a pole face of each magnetic bearing element as shown in figure 9. For more information on this sensor see reference 12. Bias current is provided in each loop by an offset which is introduced at the noninverting input of the feedback amplifier. In figure 8 the upper and lower loops are connected in a differential configuration so that a positive input will add to the bias voltage

provided by the offset input to the upper loop and subtract from the offset input to the lower loop. Because of the high open loop gain of the input operational amplifier, the flux remains essentially constant over the operating gap range for a given input and offset voltage. To illustrate, consider the simplified representation of a given flux feedback loop presented in figure 10. In this figure, the open loop gain of the input operational amplifier is combined with the closed loop gain of the inner current feedback loop and defined as G_F. The gain from flux input to Hall element voltage output is defined as K_H and the gain of the Hall element voltage amplifier is defined as G_H. If the resistance of the bearing element coil is R_c, the inductance is L_c, and the current through the coil is i, then the voltage across the coil, V_c, can be written as

$$V_c = iR_c + L_c \frac{di}{dt} = iR_c(1 + \tau_c s) \tag{22}$$

where $\tau_c = \dfrac{L_c}{R_c}$. The current in the coil becomes

$$i = \frac{V_c}{R_c(1 + \tau_c s)} \tag{23}$$

From equation (6) the flux, ϕ, is

$$\phi = K_\phi \frac{i}{G} \tag{24}$$

where $K_\phi = \dfrac{\mu_o NA}{2}$. Substituting for i, the flux as a function of voltage across the coil becomes

$$\phi = \frac{K_\phi V_c}{GR_c(1 + \tau_c s)} \tag{25}$$

In terms of the error voltage ϵ at the summing junction, V_c becomes

$$V_c = \epsilon G_F = (E_i - E_o)G_F \tag{26}$$

The Hall element voltage, V_H, can be written as

$$V_H = K_H \phi \tag{27}$$

7

E_o then becomes

$$E_o = K_H G_H \phi \tag{28}$$

and V_c becomes

$$V_c = E_i G_F - K_H G_H G_F \phi \tag{29}$$

Substituting equation (29) into equation (25) results in

$$\phi = \frac{K_\phi (E_i G_F - K_H G_H G_F \phi)}{GR_c(1 + \tau_c s)} \tag{30}$$

Rearranging and collecting terms results in

$$\frac{\phi}{E_i} = \frac{K_\phi G_F}{K_\phi K_H G_H G_F + GR_c(1 + \tau_c s)} \tag{31}$$

which can be further simplified to

$$\frac{\phi}{E_i} = \frac{1}{K_H G_H + \dfrac{GR_c(1 + \tau_c s)}{K_\phi G_F}} \tag{32}$$

Since G_F, the open loop gain of the operational amplifier times the closed loop gain of the current loop, is much larger than the other terms in the equation, then the approximation

$$\frac{\phi}{E_i} = \frac{1}{K_H G_H} \tag{33}$$

can be made, which shows the flux to be independent of gap position.

The flux feedback configuration shown in figure 8 can also be used for a permanent magnet bias flux actuator. In a permanent magnet bias flux system, the input offset adjustment for each loop can be used to null out the offset introduced by the permanent magnets to establish a baseline about which the feedback loops operate and to provide fine adjustment between upper and lower bias flux.

Baseline is established by adjusting the input offsets so that the upper and lower loops have zero error inputs with the suspended element in the center of the gap and the flux command input grounded. If the upper and lower permanent magnets are not exactly the same strength, one loop may have to have a small offset adjusted in to compensate for the difference.

TEST RESULTS

This section presents test results for the implementation of the flux feedback approach for magnetic actuator control which was described in the previous section. The tests were performed using the microcomputer controlled magnetic bearing test fixture which is described in detail in reference 13. The test fixture is shown in figure 11, and the placement of the Hall-effect sensors can be seen in figure 9. The magnetic bearing gap, with the equivalent suspended element centered between bearing elements, was set at 0.100 inch. As described in reference 13, the magnetic bearing elements have the same dimensions as the original magnetic bearing elements delivered with the laboratory model AMCD (ref. 2). Unlike the original elements, however, the test fixture elements contain no permanent magnet material and use SAE 1010 soft steel as core material. The area of each pole face is one square inch and the number of turns per element is 184. Initial adjustments on the system were made with the equivalent suspended element centered. These included adjusting the bias currents for each coil to 1.0 Amp. and adjusting the gain of the Hall-effect amplifiers to produce an output voltage of 1.0 volt before the flux feedback loop was closed. With these parameters, equation (18) can be used to compute the theoretical gain of the actuator. The bias flux, ϕ_o, can be calculated from equation (6), $\bar{K}$ is defined by equation (9), and ϕ_c is defined by equation (33). $K_H G_H$ can be determined from equation (28) by substituting ϕ_o for ϕ and 1.0 volt for E_o. Making all the appropriate substitutions into equation (18) and simplifying results in

$$\frac{F_T}{E_i} = \mu_o A N^2 \left(\frac{I_o}{G_o}\right)^2 \tag{34}$$

Using the values given above, the theoretical gain is calculated to be $F_T/E_i = 0.96$ lb/v. The data were taken over a gap range of 0.060 inch (0.030 to -0.030) in increments of 0.010 inch. This gap range is considered to be typical for an AMCD type application (see ref. 14). The command voltage at each gap position was varied from -1.0 to 1.0 volts in increments of 0.1 volt. The data were smoothed by applying a first order, least-squares curve fit. A plot of force versus force command for the center position and ±0.030 inch is shown in figure 12. As can be seen from the figure, there is a slight shift in slope at the outer gap positions. The remainder of the data fit between these extremes. The small change in slope, or gain, is due to the effect of leakage flux which has increasing effect as the gap approaches zero for a given bearing element. A plot of gain versus gap is shown in figure 13. In this figure, the solid line is the mean value of the gain and the data points represent the gain calculated at a given gap position. The mean value of the gain is 1.03, which compares favorably with the theoretical gain of 0.96, and the standard deviation of the gain is 0.021. Figures 14 and 15 present plots of force versus gap at fixed force commands of -0.2, -0.4, and 0.2, 0.4 volts, respectively. The solid lines represent mean values for a given force command and the data points are actual values measured at a given gap position. It should be noted at this point

9

that as the force command approached ± 1.0 volt, which means that the current in a given coil approached zero current crossover, there was a slight shift in gain similar to that due to leakage flux at smaller gaps. In a given application, the magnetic bearing elements can be designed to minimize leakage flux over a desired gap range, and they would also be sized so that normal operation would be well within the limits of the bias currents (ref. 11).

CONCLUDING REMARKS

A magnetic bearing control approach which uses flux feedback to produce a linear transfer characteristic between force command and force output over a large gap range has been described and test results for an implementation of the approach using a laboratory model magnetic bearing actuator have been presented. The magnetic bearing actuator consists of elements similar to those used in a laboratory model Annular Momentum Control Device (AMCD). Results obtained from tests using the flux feedback actuator generally showed close agreement with theoretical predictions. Using data taken over a gap range of 0.060 inch, the mean value of the gain was calculated to be 1.03 lb/v with a standard deviation of 0.021 compared to a theoretical value of 0.96 lb/v.

The flux feedback approach which was implemented uses bias currents to produce bias flux. This was due primarily to the fact that there is more flexibility in setting test parameters with bias currents. However, since the data that were presented were for fixed bias currents, they are directly applicable to an actuator with permanent magnet flux bias. In most applications, permanent magnet flux bias would be the preferred approach because of power consumption and actuator heating issues.

REFERENCES

1. Anderson, Willard W.; and Groom, Nelson J.: The Annular Momentum Control Device (AMCD) and Potential Applications. NASA TN D-7866, March 1975.

2. Ball Brothers Research Corporation: Annular Momentum Control Device (AMCD). Volumes I and II. NASA CR-144917, 1976.

3. Groom, Nelson J.: Description of a Laboratory Model Annular Momentum Control Device (AMCD). NASA CP-2346, pp. 157-167, November 1984.

4. Groom, Nelson J.; and Terray, David E.: Evaluation of a Laboratory Test Model Annular Momentum Control Device. NASA TP-1142, March 1978.

5. Groom, Nelson J.; and Waldeck, Gary C.: Magnetic Suspension System for Laboratory Model Annular Momentum Control Device. Presented at the AIAA Guidance and Control Conference, Boulder, Colorado, August 1979. (Available as AIAA paper 79-1755).

6. Groom, Nelson J.; and Miller, James B.: A Microprocessor - Based Table Lookup Approach for Magnetic Bearing Linearization. NASA TP-1838, 1981.

7. Anderson, Willard W.; Groom, Nelson J.; and Wooley, Charles T.: The Annular Suspension and Pointing System. Journal of Guidance and Control, vol. 2, no. 5, September-October 1979, pp. 367-373.

8. Groom, Nelson J.: Overview of Magnetic Bearing Control and Linearization Approaches for Annular Magnetically Suspended Devices. NASA CP-2346, pp. 297-306, November 1984.

9. Groom, Nelson J.: Analytical Model of an Annular Momentum Control Device (AMCD) Laboratory Test Model Magnetic Bearing Actuator. NASA TM-80099, August 1979.

10. Sperry Flight Systems: Magnetic Suspension System for an Annular Momentum Control Device (AMCD). NASA CR-159255, December 1979.

11. Cunningham, D. C.; Gismondi, T. P.; and Wilson, G. W.: System Design of the Annular Suspension and Pointing System (ASPS). Presented at the AIAA Guidance and Control Conference, Palo Alto, California, August 1978. (Available as AIAA paper 78-1311).

12. Texas Instruments, Inc.: TL3103I, TL3103C Linear Hall-Effect Sensors. May 1985.

13. Groom, Nelson J.; and Poole, William L.: Description of a Magnetic Bearing Test Fixture. NASA TM-89081, March 1987.

14. Groom, Nelson J.; Woolley, Charles T.; and Joshi, Suresh M.: Analysis and Simulation of a Magnetic Bearing Suspension System for a Laboratory Model Annular Momentum Control Device. NASA TP-1799, March 1981.
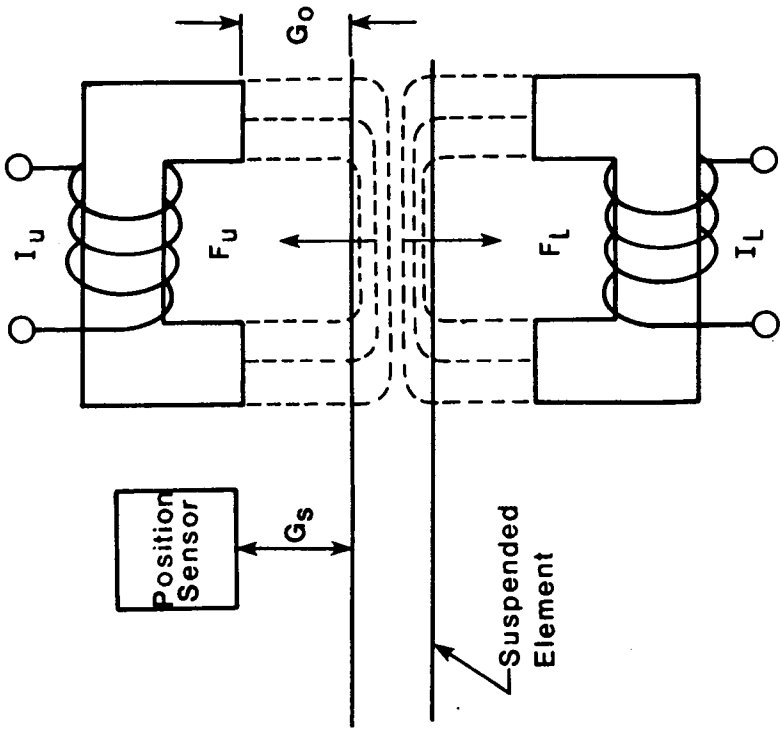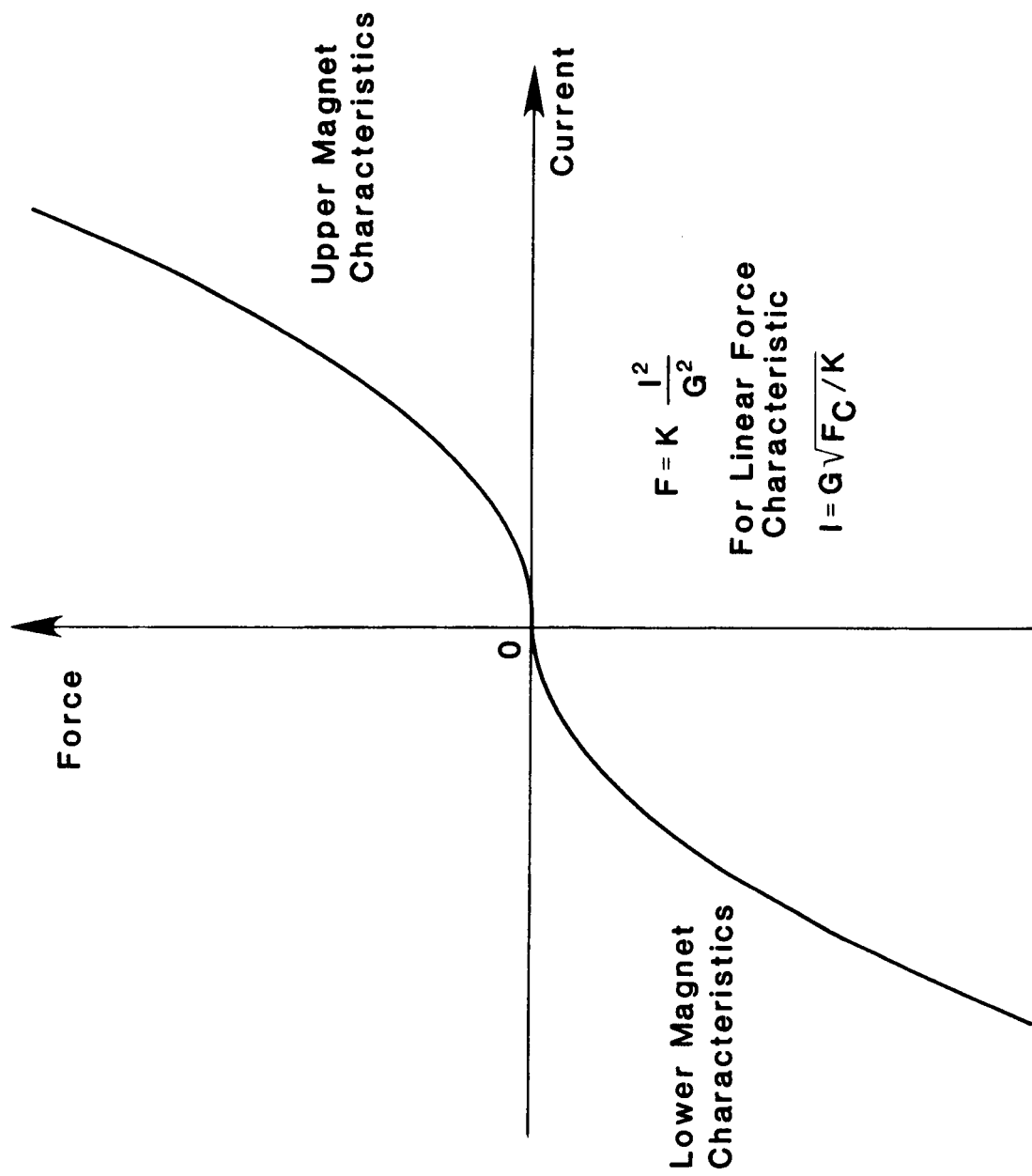
Figure 1.-Magnetic bearing actuator

Upper Magnet Characteristics

Current

$$F = K\ \frac{I^2}{G^2}$$

For Linear Force Characteristic

$$I = G\sqrt{F_C/K}$$

Force

0

Lower Magnet Characteristics

Figure 2.-Force current characteristic of a magnetic actuator with individual element control

$$F_u = K \frac{I_u^2}{G_u^2} \quad , \quad G_u = (G_o - G)$$

$$I_u = \frac{1}{G_o} \sqrt{\frac{F_c}{K}} \ (G_o - G)$$

$$F_u = \overline{K} \ F_c$$

G From Sensor

$$F_L = K \frac{I_L^2}{G_L^2} \quad , \quad G_L = (G_o + G)$$

$$I_L = \frac{1}{G_o} \sqrt{\frac{F_c}{K}} \ (G_o + G)$$

$$F_L = \overline{K} \ F_c$$
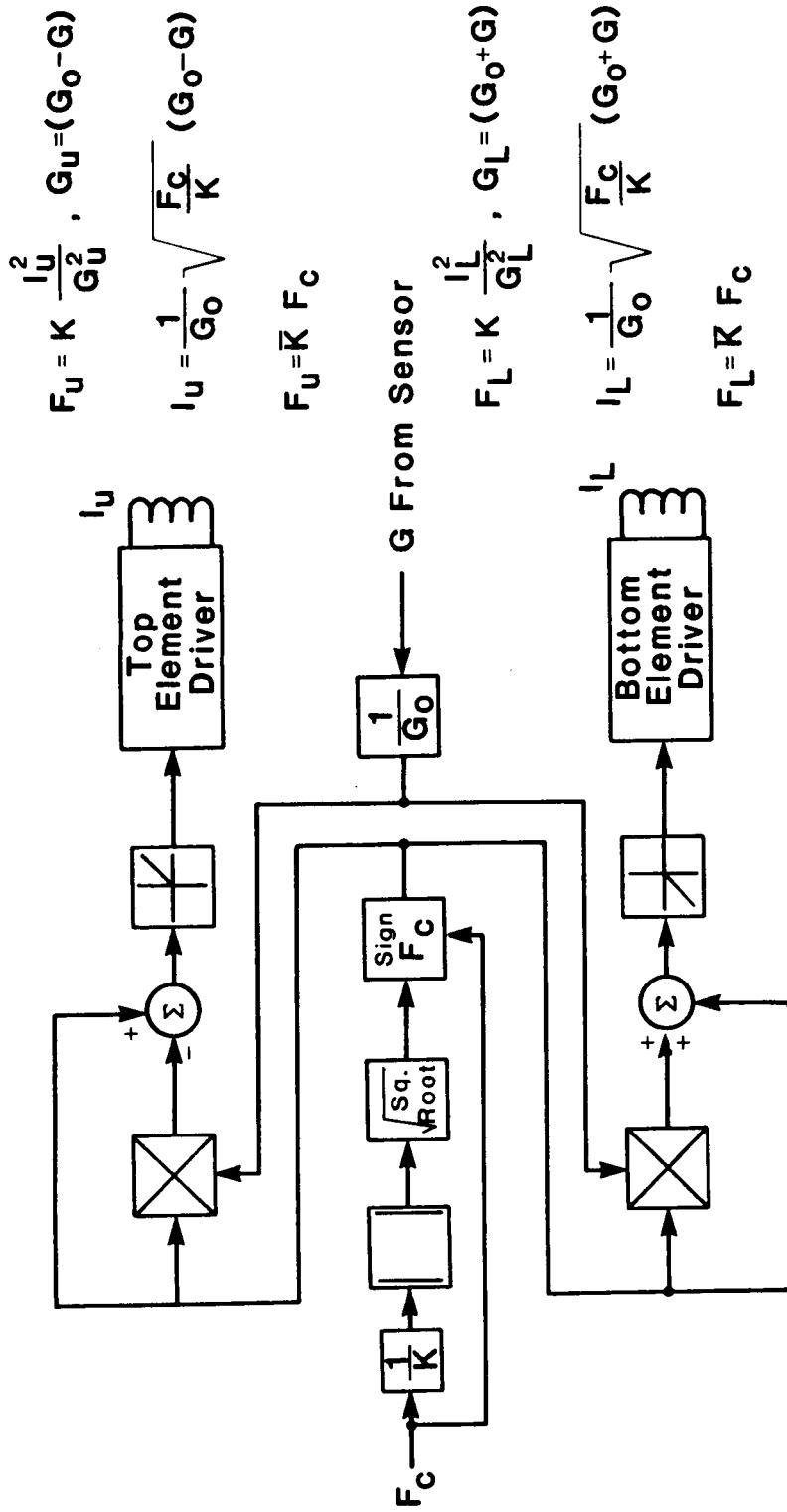
Figure 3.-Analog solution of the force equation for individual element control
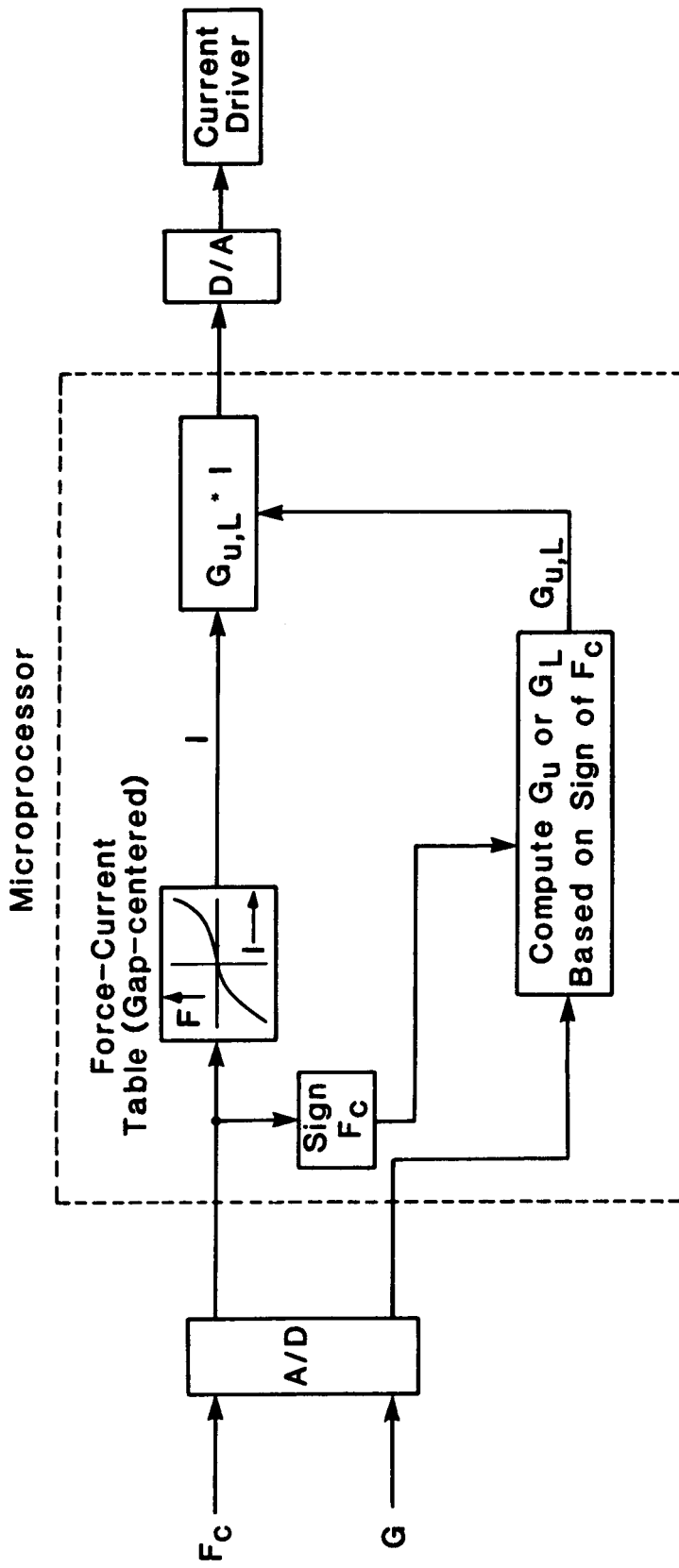
Figure 4.-Table look-up approach for individual element control
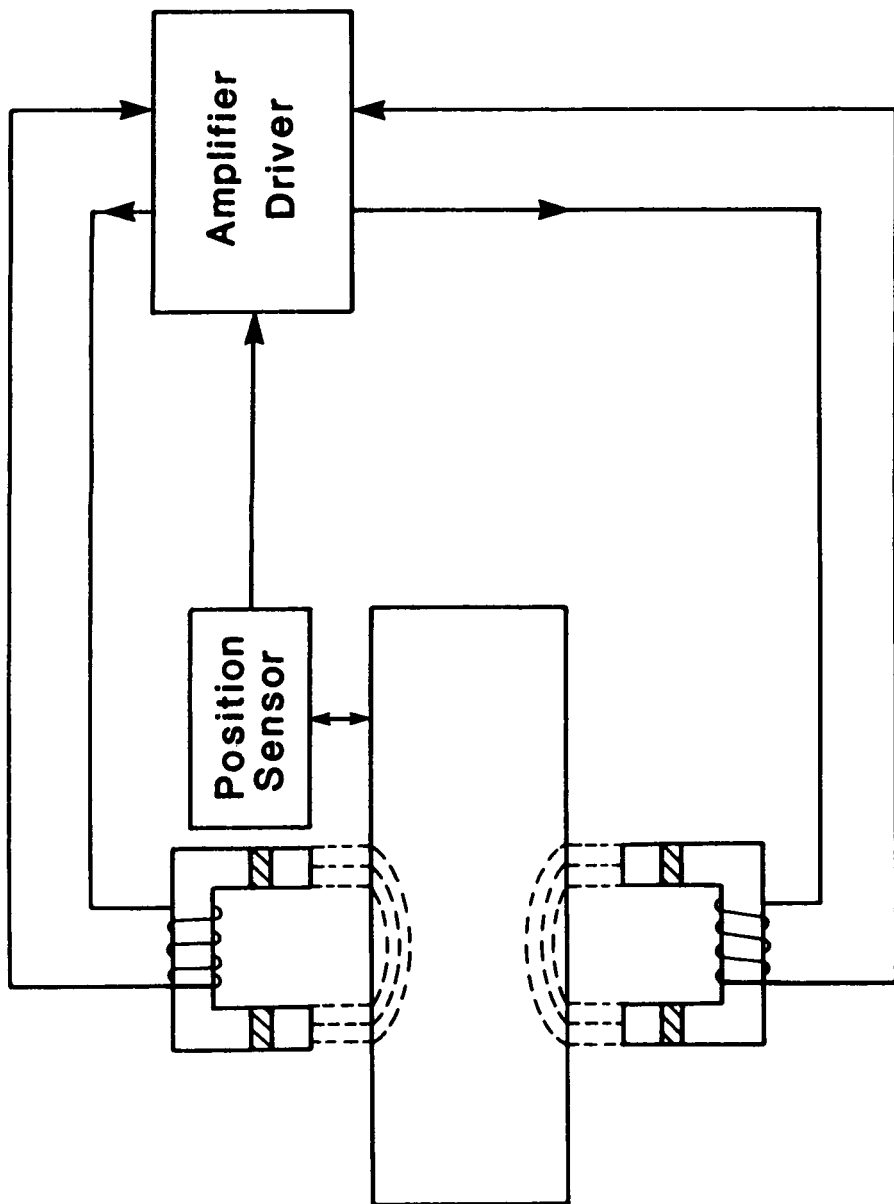
Figure 5.-Permanent magnet flux-biased magnetic actuator
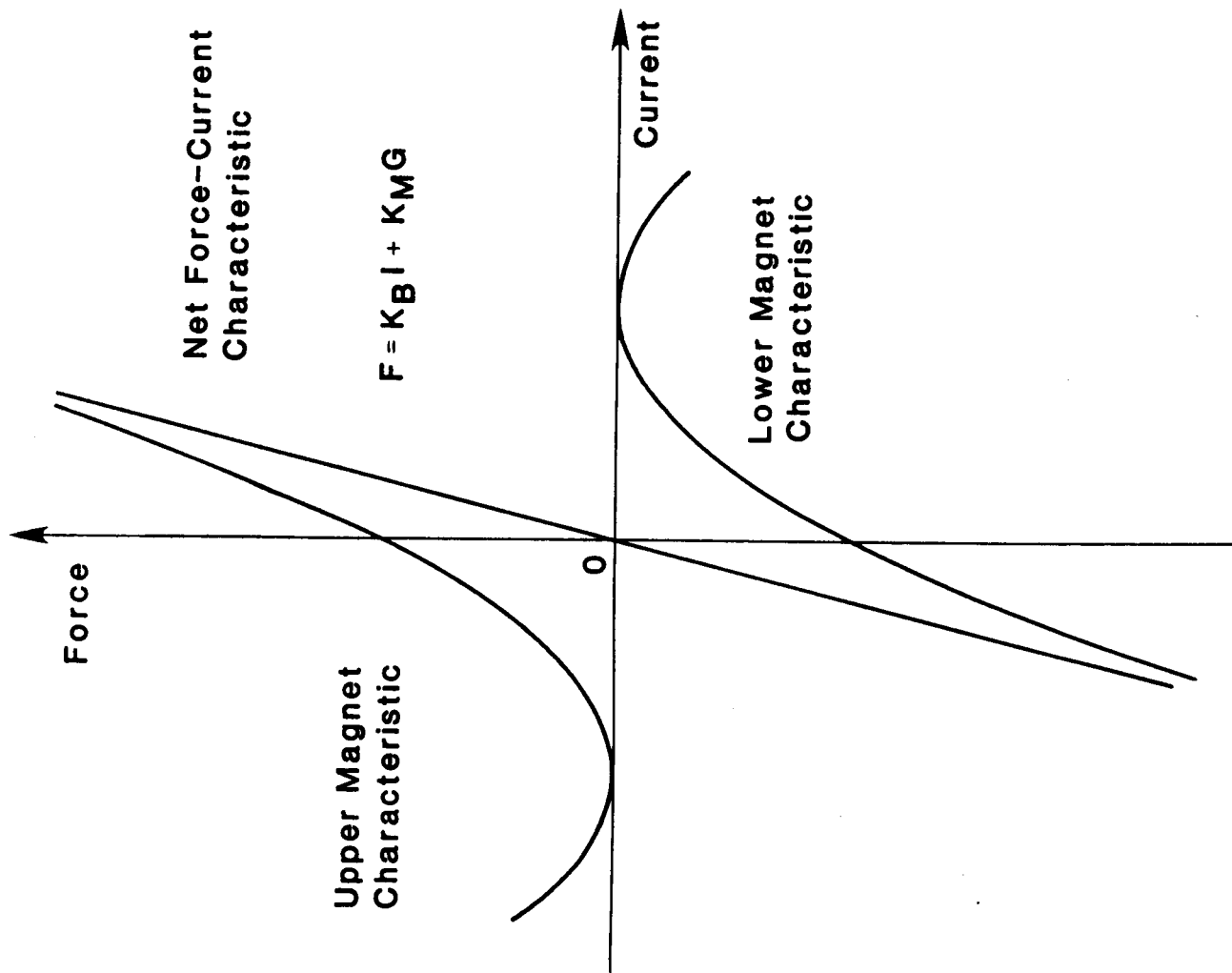
Figure 6.-Force-current characteristic of a permanent magnet flux-biased magnetic acutator

The figure is labeled with:
- Force (vertical axis)
- Current (horizontal axis)
- Net Force-Current Characteristic
- $F = K_B I + K_M G$
- Upper Magnet Characteristic
- Lower Magnet Characteristic
- O (origin)

17
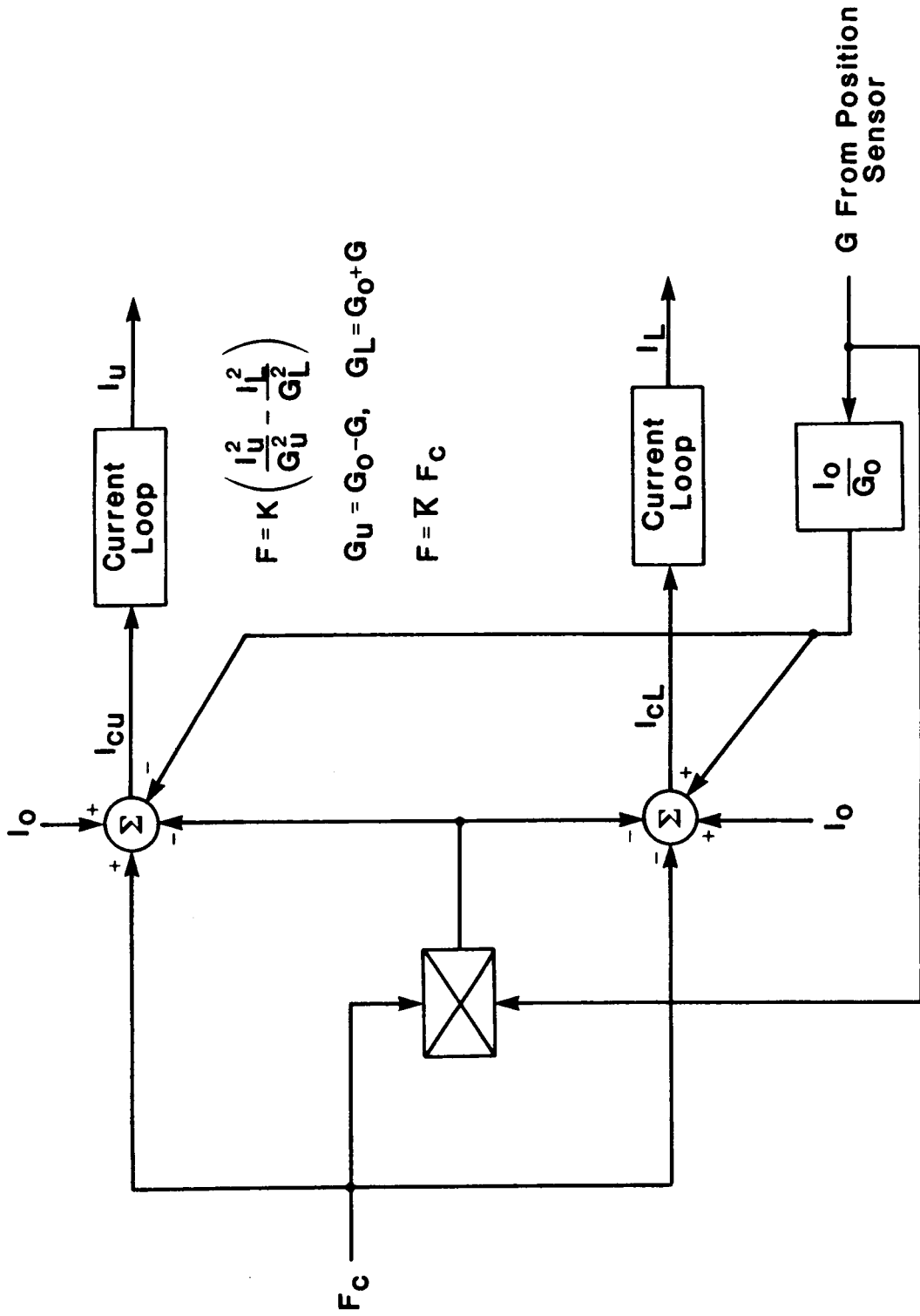
Figure 7.-Variable biased current approach for magnetic actuator control

$$F = K\left(\frac{I_u^2}{G_u^2} - \frac{I_L^2}{G_L^2}\right)$$

$$G_u = G_o - G, \quad G_L = G_o + G$$

$$F = K\ F_c$$

18
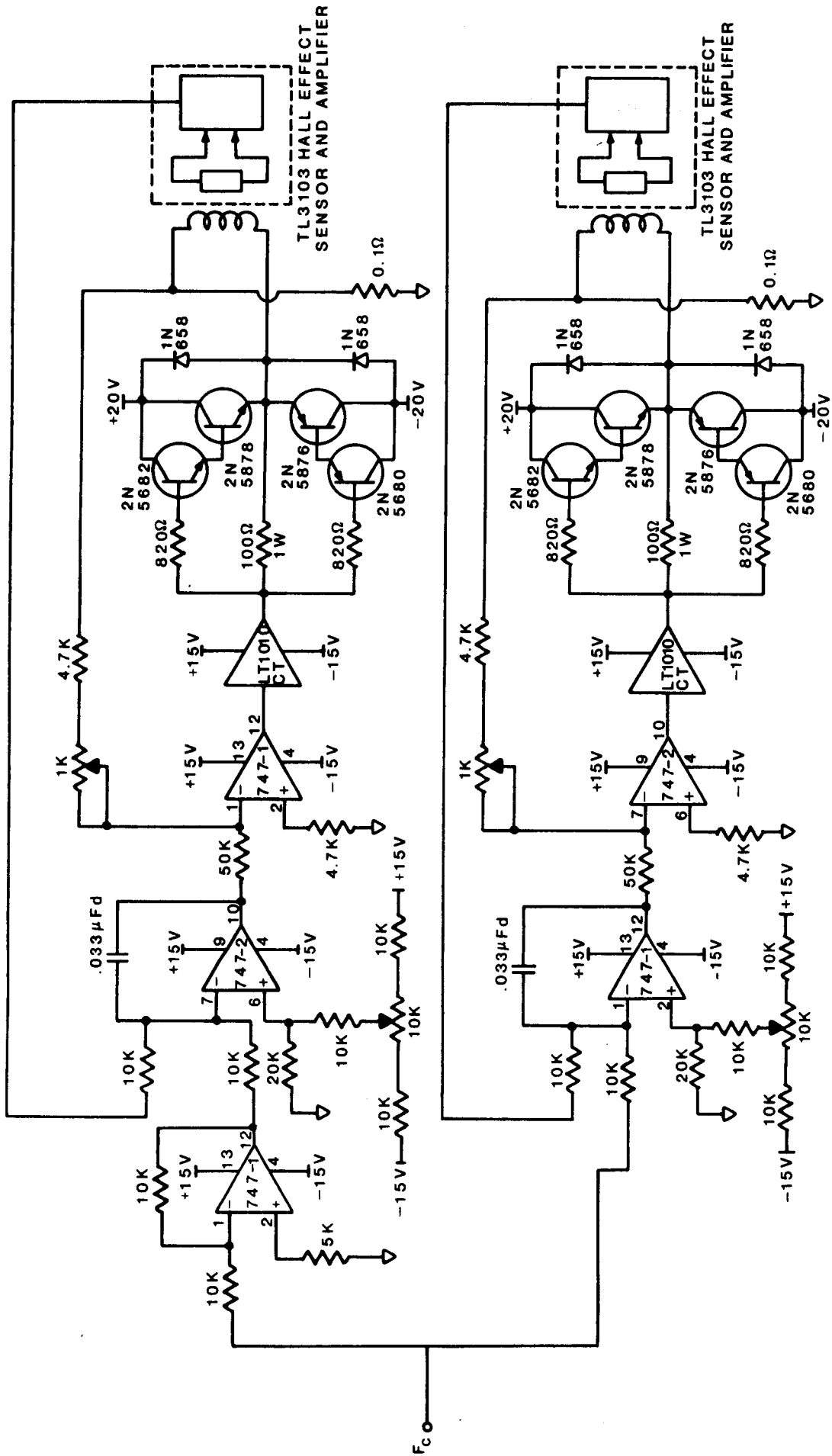
Figure 8.-Implementation of flux feedback approach

19
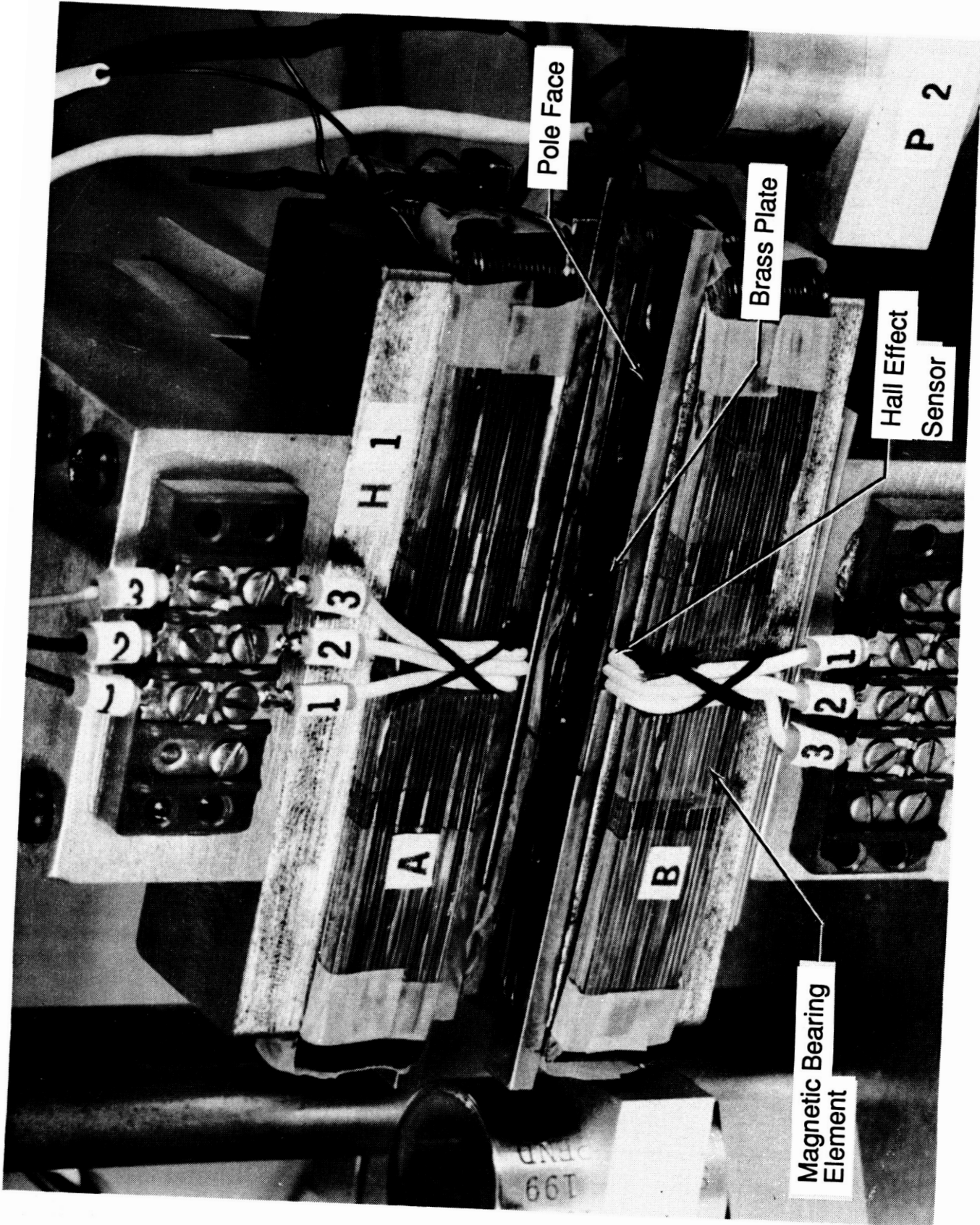
Figure 9.-Magnetic bearing actuator
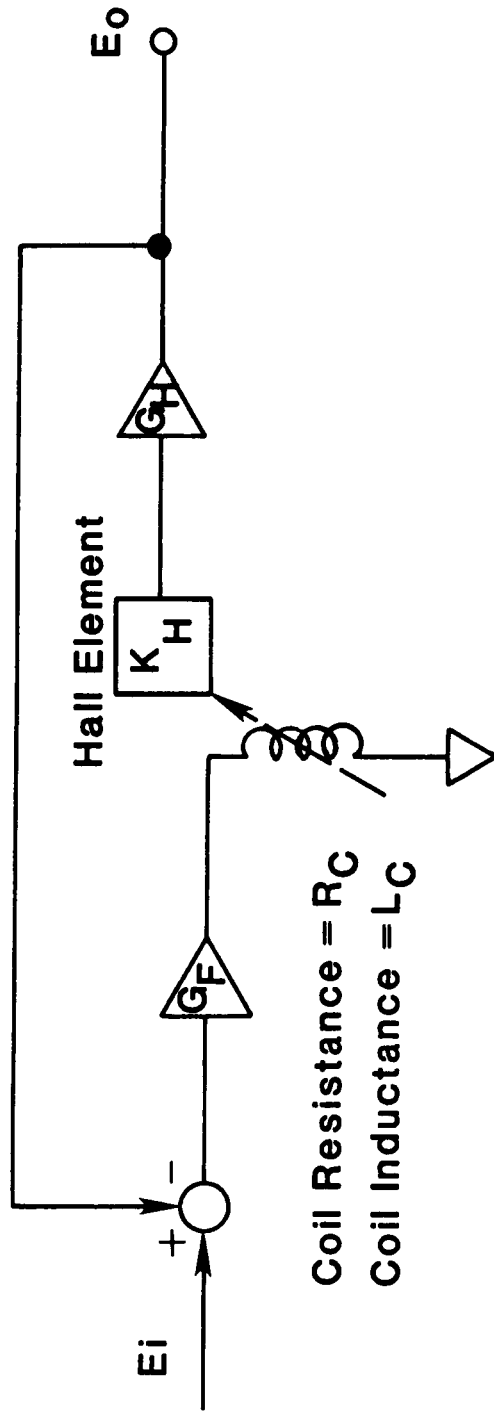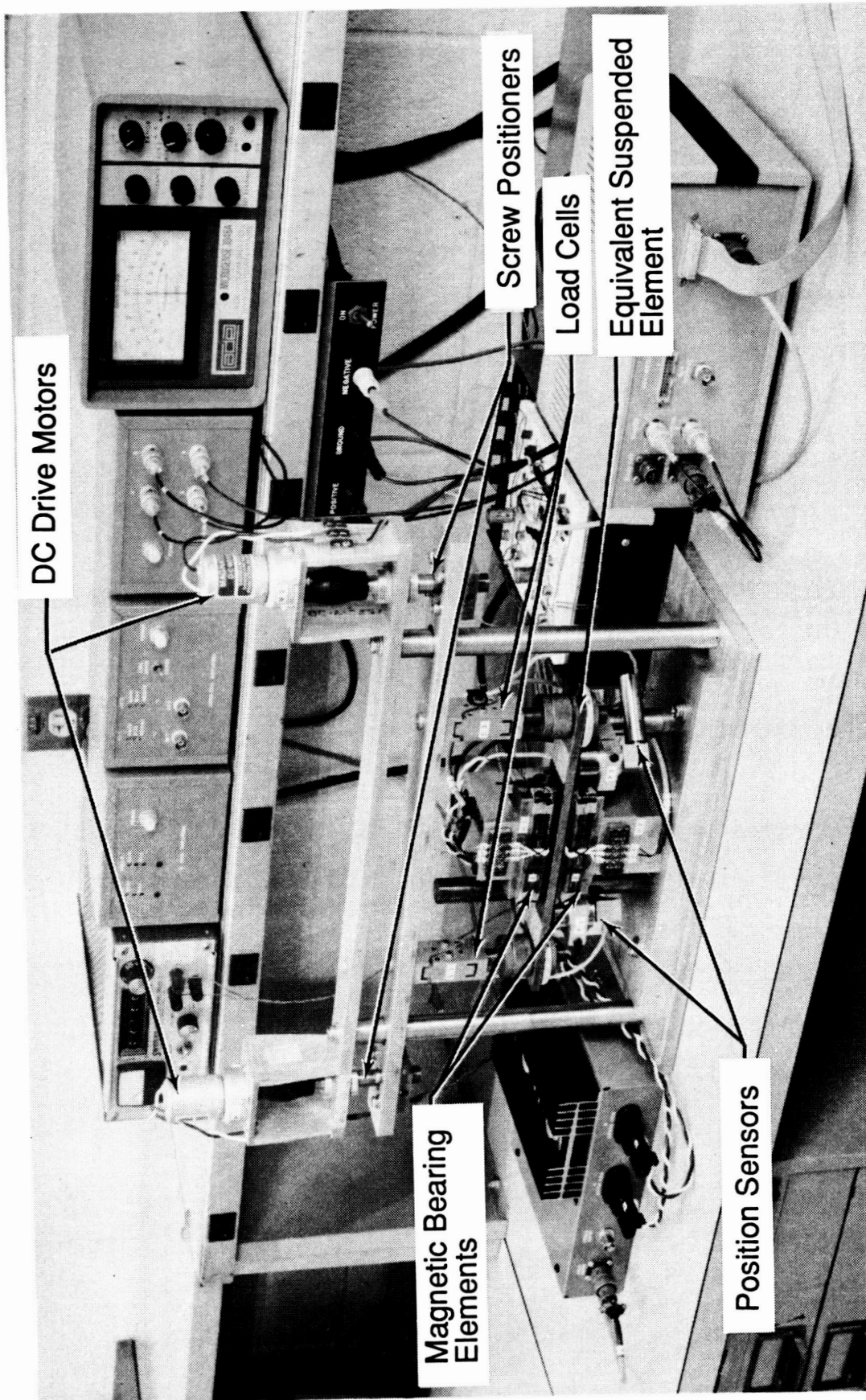
Figure 10.-Simplified schematic of flux feedback loop

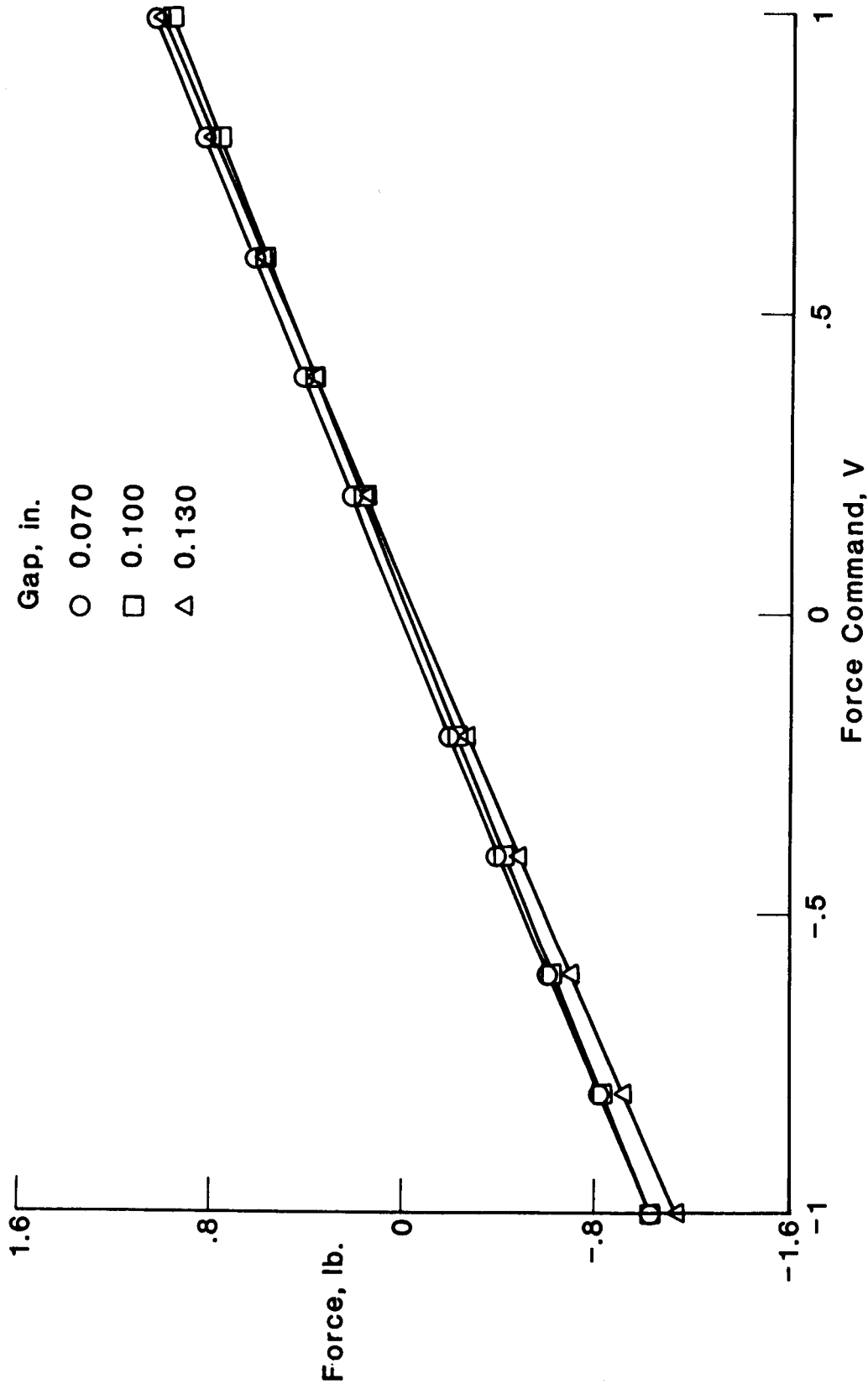Figure 11.-Magnetic bearing test fixture

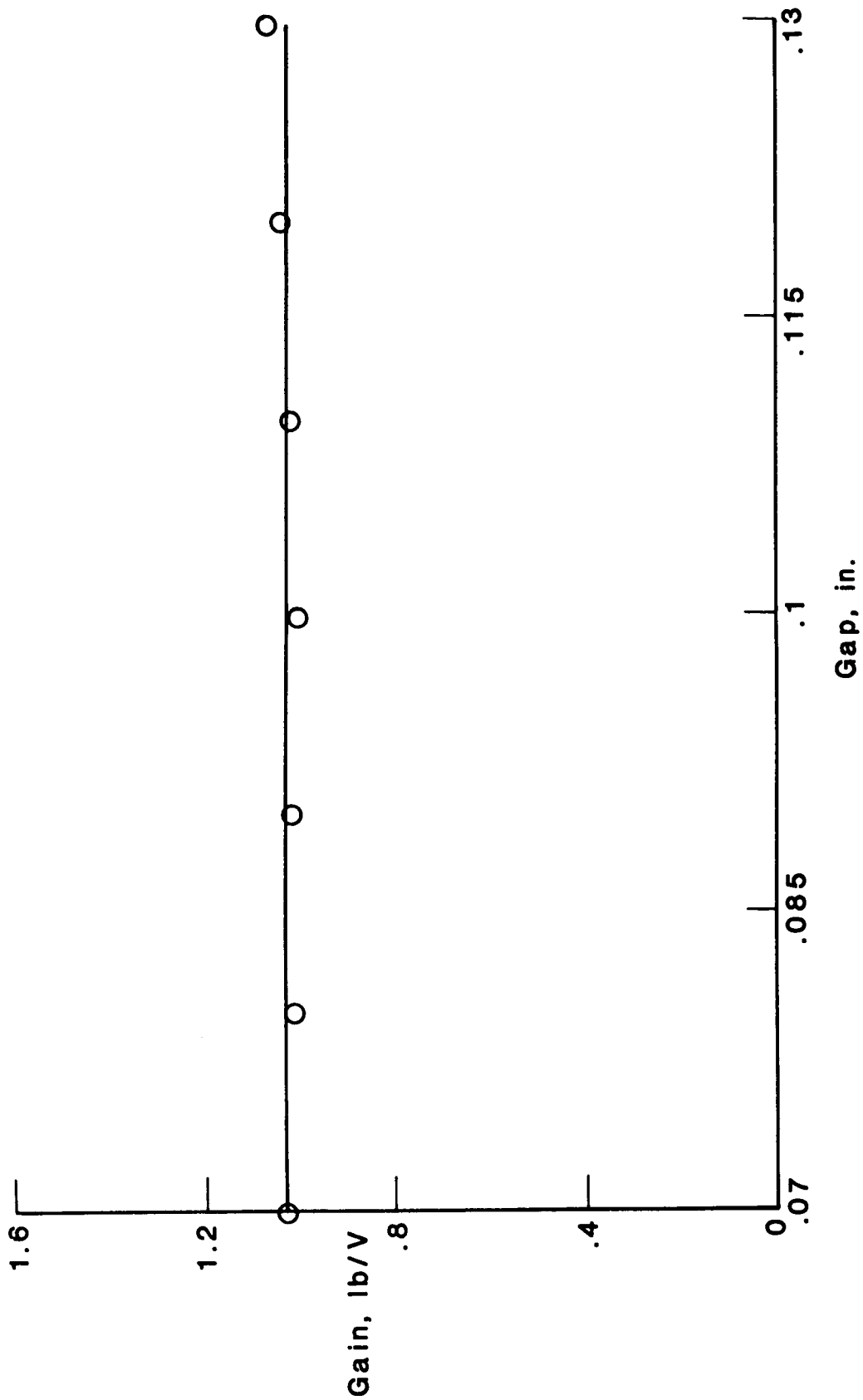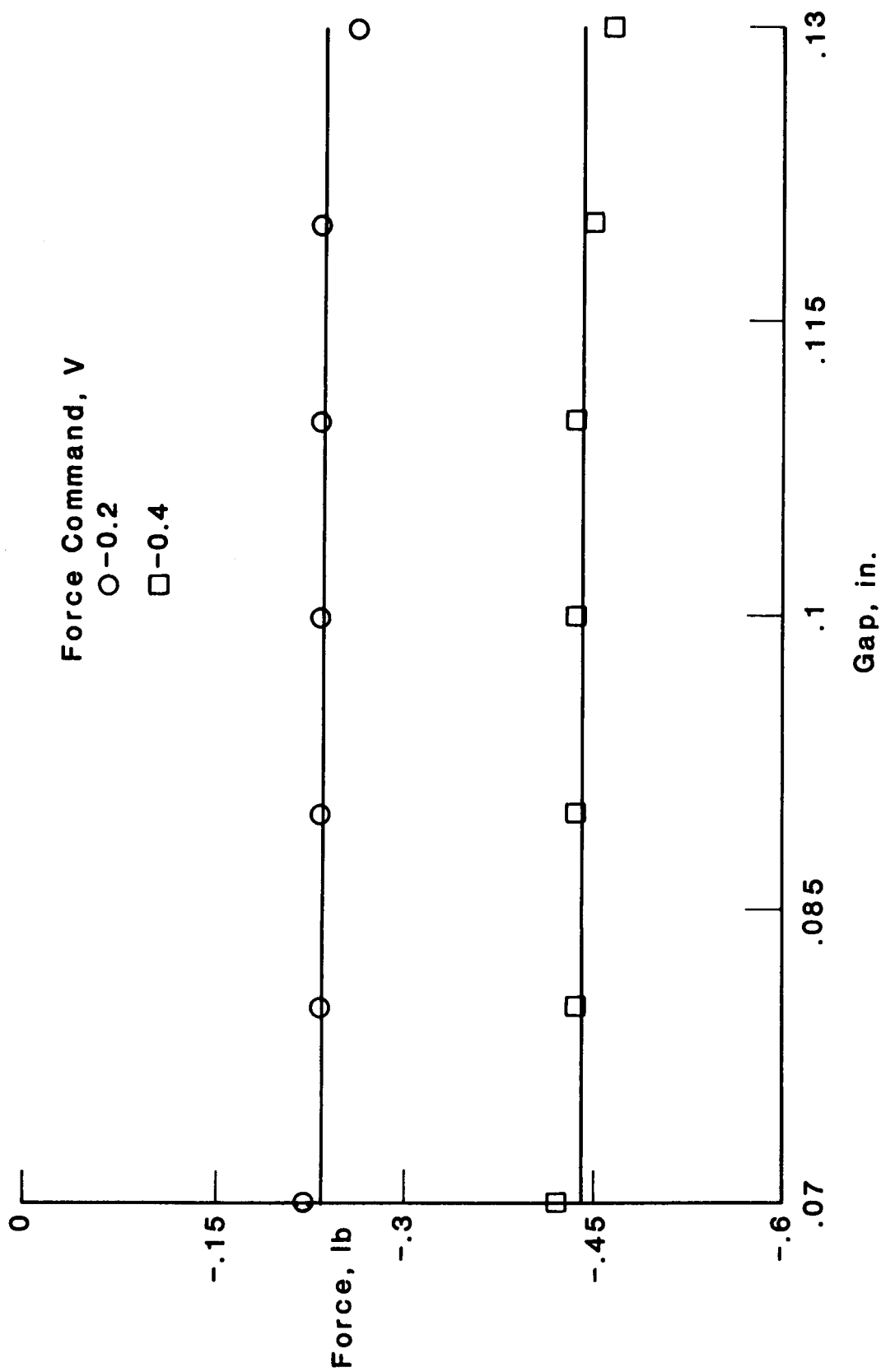Figure 12.-Force vs. force commands at fixed gaps

Figure 13.-Gain vs. gap

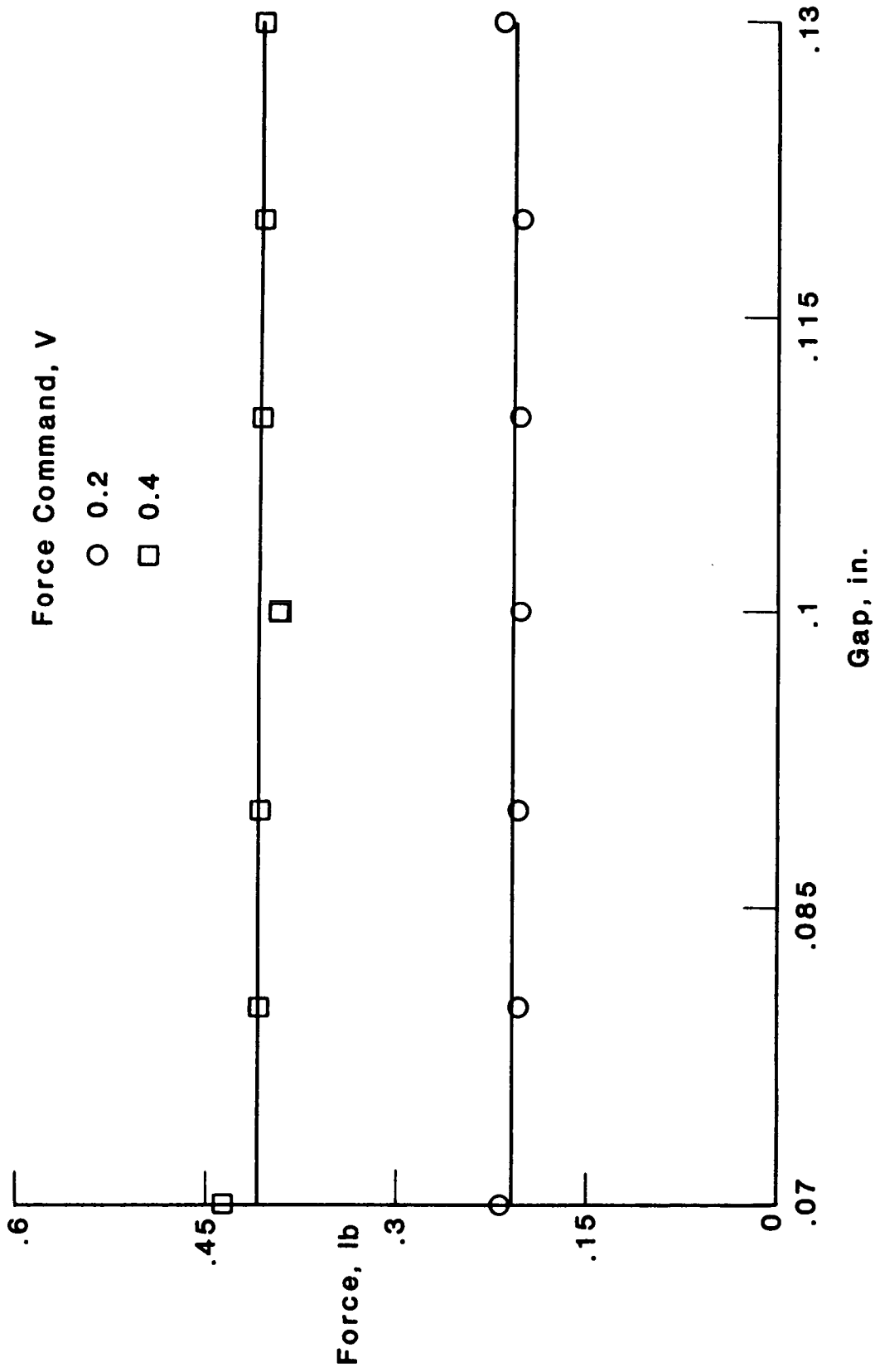Figure 14.-Force vs. gap at fixed force commands
(negative values)

Figure 15.-Force vs. gap at fixed force commands (positive values)

NASA

Report Documentation Page

1. Report No. NASA TM-100672	2. Government Accession No.	3. Recipient's Catalog No.
4. Title and Subtitle A Magnetic Bearing Control Approach Using Flux Feedback		5. Report Date **March 1989**
		6. Performing Organization Code
7. Author(s) Nelson J. Groom		8. Performing Organization Report No.
		10. Work Unit No. 585-01-61-08
9. Performing Organization Name and Address NASA Langley Research Center Hampton, VA 23665-5225		11. Contract or Grant No.
		13. Type of Report and Period Covered Technical Memorandum
12. Sponsoring Agency Name and Address National Aeronautics and Space Administration Washington, DC 20546-0001		14. Sponsoring Agency Code

15. Supplementary Notes

16. Abstract

    A magnetic bearing control approach using flux feedback is described and test results for a laboratory model magnetic bearing actuator are presented. Test results were obtained using a magnetic bearing test fixture, which is also described. The magnetic bearing actuator consists of elements similar to those used in a laboratory test model Annular Momentum Control Device (AMCD).

17. Key Words (Suggested by Author(s)) Annular Momentum Control Device Magnetic Bearing Actuator Flux Feedback Magnetic Actuator Control	18. Distribution Statement Unclassified-Unlimited Subject Catagory 31		
19. Security Classif. (of this report) Unclassified	20. Security Classif. (of this page) Unclassified	21. No. of pages 27	22. Price A03